Physical and Mathematical Modeling of non Transferred Plasma Torches

R. C. Favalli, R. N. Szente *
Departamento de Física Aplicada
Instituto de Física da Universidade de São Paulo
P.O. Box 66318 - Cep 05315-900, São Paulo, Brazil

Received August 14, 1997

The main objective of this work is to obtain temperature and velocity profiles of the plasma jet, including the electric arc region, generated by non transferred plasma torches. The profiles are obtained from a numerical solution of the conservation equations which were used to describe the plasma flow. This modeling approach will help the development and optimization of plasma torches, saving time and reducing costs of an alternative empirical development; it could also give some insight on the phenomena occuring inside the torch. Fluid mechanics models for laminar and turbulent flows were adopted to simulate the plasma inside and outside the torch. Patankar's control volume method was chosen to solve the resulting coupled differential equations. The method is very stable and requires less computational time than higher order methods, although it can be less accurate for some applications. A computer code was developed to simulate the jet flow of a plasma torch. The results obtained from this program compared very well with published ones, corroborating the assumptions of the present model and the numerical method. Temperature and velocity profiles for a plasma torch with dimentions and operating conditions similar to the ones used in industrial applications of spraying were generated and analyzed. The plasma torch simulated had an electric arc of $100A$, plasma gas flow rate of $20\ l/min$, cross section of $5.2mm$ and anode length of $13mm$.

I. Introduction

Thermal plasmas have been employed in an increasing number of industrial applications since their first development in the early 50's. Typical applications of this technology include materials processing (spraying, production of ceramic parts, synthesis of compounds such as titaniun dioxide, silicon carbide, silicon nitride, superconductors) and metallurgy (blast furnaces, production of special steel and ferroalloys, cutting, recovery of metal fines). In the last five years, thermal plasmas have been extensively employed to treat residues or remediate enviromental problems such as hospital waste, destruction of toxic materials, vitrification of asbestos, remelting of incineration ashes, treatment of galvanic sludges, mercury contaminated soils and many others [1-3].

Thermal plasmas are normally generated in an equipment called plasma torch which consists essentially of two electrodes (cathode and anode); an electric arc is mantained between the electrodes. A certain amount of gas is injected into the torch (in principle any gas can be used) receiving energy from the arc and generating the thermal plasma.

A specific torch design and operating conditions are normally needed for the different industrial application of this technology. This normally implies an empirical development of the equipment, resulting in high costs and long development period for the construction, modification and tests of the specific equipment.

A possible alternative for reducing the development costs of a plasma torch is to understand the phenomena involved in the torch operation and, using mathematical models and numerical schemes, solve the resulting equations. Not only will this approach reduce the time spent for developing the torch, but will reduce the direct costs involved in an empirical development. The

*To whom correspondence should be addressed

resulting physical and mathematical models of the torch will hopefully be used for different applications, simulating different sets of operating conditions and torch geometries.

In this work we present a physical and mathematical modeling of a non transferred plasma torch. The geometry of the plasma torch used in the simulations is described below. The models adopted to simulate the jet flow in the plasma torch and the results obtained from the computer program are shown after the description of the torch. The last section of the paper presents a summary of the main discussed aspects.

II. Non Transferred Plasma Torch

There are different types and geometries of plasma torches. The two main classes of plasma torches are the so called transferred and non transferred torches. In the former, the electric arc used to generate the plasma is mantained between one electrode of the torch (normally the cathode) and a piece of metal (or another conducting material) that one wants to cut or melt, located outside the torch. Those torches are typically used for metallurgical processes such as ferroalloy production or tundish heating. The other type, the non transferred plasma torches, employs the two electrodes of the torch in order to mantain the electric arc, i.e., the electric arc strikes between the two electrodes of the torch and it is kept inside the torch. These torches are normally used for spraying, production of advanced materials, and the treatment of hazardous wastes. In this work we studied the non transferred plasma torch although the computer code developed can be easily adapted to simulating transferred torches.

The plasma torch simulated in this work is based on a previous torch developed for the processing of materials and for treating industrial residues [4]. The former torch had a central injection of particles (through the cathode) and an external magnetic field was used to rotate the arc. We modeled here a more generic and simpler plasma torch, similar to the ones used in spraying (coating), without the central injection of particles and the external magnetic field. However the computer code developed here presents great flexibility, allowing easy and fast modifications in order to simulate other types of plasma torches as mentioned before.

A schematic diagram of the plasma torch modeled here is given in Fig.1. An electric arc is mantained between the two electrodes (cathode and anode); the gas passes through the space between the electrodes and it is heated by the arc, forming the plasma jet.

Typical power levels of plasma torches used for spraying are between 10 and $100kW$. Argon is normally employed as the plasma gas since it is an easily ionized gas and it does not react with the material being treated or sprayed. The overall length of those torches varies between 5 and $40cm$, with an external diameter between 1 and $10cm$; dimensions of the torch are normally function of the power level of the equipment.

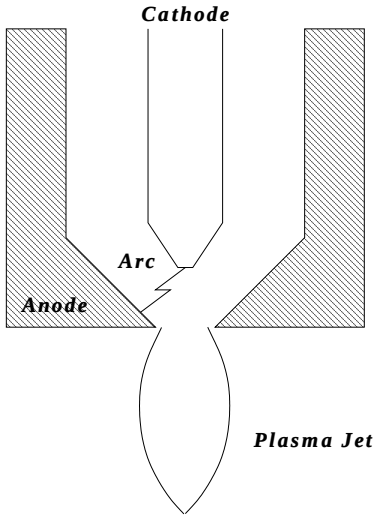

Figure 1. Schematic representation of the plasma torch modeled.

III. Theory

The physical and the mathematical models developed in this work as well as the numerical method chosen to solve the set of the resulting governing equations are presented below, followed by the computational domain and boundary conditions necessary for solving the equations and simulating the plasma jet.

III.1 Physical and Mathematical Modeling

Physical modeling of plasma torches commonly consider only the jet exiting the torch, assuming temperature and velocity profiles at the exit of the torch as boundary conditions [5,6]. However, characterization of the plasma jet temperature and velocity inside the torch can provide important information on the phenomena occurring in this region with consequences on the whole jet development. The physical model developed in this work takes into account the cold gas at the torch entrance region, the electric arc region and the free boundary region (the expansion region of the

plasma jet). This model is based on the following assumptions:

- The plasma is optically thin, i.e., the black body radiation emmited is not reabsorbed by the plasma;
- The arc is in local thermodynamic equilibrium (L.T.E.), i.e., all plasma components (electrons, ions and neutrons) have the same temperature and this condition prevails all over the plasma column, from the cathode to the anode;
- The heat dissipation due to viscosity is negligible because it is composed by second order terms;
- The gravity effects are negligible due to the high Froude number ($\approx 3 \times 10^6$);
- The arc is assumed to be steady and rotationally symmetric.

These assumptions are commonly employed in plasma torch simulations [7-10].

The plasma jet is considered here to be a fluid, instead of a statistical collection of particles (Boltzmann approach) and therefore the behavior of the plasma can be described using equations of state and conservation of mass, momentun, energy and current.

The set of differential equations used to describe the physical model can be represented by a general transport equation.

$$\frac{1}{r}\frac{\partial}{\partial r}(r\rho v\vartheta) + \frac{\partial}{\partial z}(\rho u\vartheta) = \frac{1}{r}\frac{\partial}{\partial r}\left(r,\ _{\vartheta}\frac{\partial \vartheta}{\partial r}\right) + \frac{\partial}{\partial z}\left(,\ _{\vartheta}\frac{\partial \vartheta}{\partial z}\right) + S_{\vartheta} \tag{1}$$

where ϑ is the dependent variable, , $_{\vartheta}$ is the corresponding diffusion coefficient, S_{ϑ} is the source term, u and v are the axial and radial velocity components, ρ is the mass density, z and r are the coordinates at axial and radial directions. The left hand side is the convective part and the right hand side represents the diffusive part and the sources.

As mentioned before, equation 1 can represent the conservation of mass, momentum and energy of the plasma jet. The parameters of the governing equations for the plasma jet are given in Table 1.

Table 1: **Equations used for the model**

Conservation of	ϑ	, $_{\vartheta}$	S_{ϑ}
Mass	1	0	0
Axial Momentum	u	ν	$-\frac{\partial p}{\partial z} + \frac{1}{r}\frac{\partial}{\partial r}\left[r\nu\frac{\partial v}{\partial z}\right] + \frac{\partial}{\partial z}\left[\nu\frac{\partial u}{\partial z}\right] + j_r B_\theta$
Radial Momentum	v	ν	$-\frac{\partial p}{\partial r} + \frac{1}{r}\frac{\partial}{\partial r}\left[r\nu\frac{\partial v}{\partial r}\right] + \frac{\partial}{\partial z}\left[\nu\frac{\partial u}{\partial r}\right] - 2\nu\frac{v}{r^2} - j_z B_\theta$
Energy	h	$\frac{k}{C_p} + k_t$	$\frac{{j_r}^2 + {j_z}^2}{\sigma} - S_r$
Turbulent Energy	K	$\mu + \frac{\mu_t}{Pr_k}$	$G - \rho\varepsilon$
Dissipation Rate of K	ε	$\mu + \frac{\mu_t}{Pr_\varepsilon}$	$C_1 G\frac{\varepsilon}{K} - \rho C_2\frac{\varepsilon^2}{K}$

In Table 1, p is the pressure, h is the specific enthalphy, C_p is the specific heat, the thermal and electrical conductivities are k and σ, respectively; ν is the effective viscosity, j_z and j_r are the axial and radial current densities, B_θ is the azimutal component of the magnetic field and S_r is the radiation heat loss. The last two equations in the Table 1 are used for the turbulence model $K-\varepsilon$ [11], where K is the kinetic turbulent energy and ε its dissipation rate; μ and μ_t are the laminar and turbulent viscosities; k_t is the turbulent thermal conductivity. C_1, C_2, Pr_k and Pr_ε are constants of the $K-\varepsilon$ model (see Table below) and G, given

$$G = 2\mu_t\left[\left(\frac{\partial v}{\partial r}\right)^2 + \frac{v^2}{r} + \left(\frac{\partial u}{\partial z}\right)^2\right] + \mu_t\left(\frac{\partial u}{\partial r} + \frac{\partial v}{\partial z}\right)^2 \tag{2}$$

is the product of the eddy viscosity and viscous dissipation terms.

The turbulent viscosity (μ_t) and the thermal conductivity (k_t) are defined using the values of K and ε obtained from the solution of their differential equa-

tions,

$$\mu_t = C_\mu \rho \frac{K^2}{\varepsilon} \quad and \quad k_t = \mu_t \frac{Cp}{Pr_t} \tag{3}$$

where C_μ and Pr_t are also constants of the turbulent model adopted in this work. These constants are presented in Table 2.

Table 2 Constant values of $K-\varepsilon$ model

C_1	C_2	C_μ	Pr_t	Pr_K	Pr_ε
1.44	1.92	0.09	0.9	1.0	1.3

Those values were suggested by Launder & Spalding [11]. According to those authors for axisymmetric jets C_μ and C_2 should be modified as follows,

$$C_\mu = 0.09 - 0.04f \quad and \quad C_2 = 1.92 - 0.0667f, \tag{4}$$

where $f = \left|\frac{\delta}{2\Delta u}\left(\frac{\partial u_0}{\partial z} - \left|\frac{\partial u_0}{\partial z}\right|\right)\right|^{0.2}$, δ is the jet diameter, u_0 is the axial velocity at the center line and Δu is the difference between the center line and the free boundary velocities.

The $K-\varepsilon$ model was chosen among several turbulence models normally used to describe turbulent flows since ε appears directly as an unknown in the K equation [12] as well as it represents nicely the characteristic of plasma flows.

The thermodynamic and transport properties of the plasma such as viscosity, density and electrical conductivity were taken initially from the literature [13] and later modified [14]. Those properties were considered to be only temperature dependent.

In the energy equation the term for the energy transfer due the to electron flow was omitted since it is considerably smaller than the other terms of the equation [15]. Enthalpy was chosen instead of temperature to guarantee the conservation of energy in the calculations [15,16]. The temperature values, used for calculating the plasma transport and thermodynamic properties were obtained using the variation of enthalpy as a function of temperature,

$$h = \int C_p dT \ . \tag{5}$$

It is necessary to take into account the current densities and the azimuthal magnetic field of the arc, considered as source terms in the governing equations. Those parameters were obtained from the current conservation equation and one of the Maxwell's equations,

$$\frac{1}{r}\frac{\partial}{\partial r}\left(r\sigma\frac{\partial \Phi}{\partial r}\right) + \frac{\partial}{\partial z}\left(\sigma\frac{\partial \Phi}{\partial z}\right) = 0 \ , \tag{6}$$

$$\frac{1}{r}\frac{\partial}{\partial r}(rB_\theta) = \mu_0 j_z \ , \tag{7}$$

where μ_0 is the permeability of the freespace, Φ is the electrical potential and σ is the electrical conductivity. The current densities are given by

$$j_z = -\sigma\frac{\partial \Phi}{\partial z} \quad and \quad j_r = -\sigma\frac{\partial \Phi}{\partial r} \ . \tag{8}$$

Equation 6 does not present the conservative form of equation 1 but it was solved by the same algorithm used for solving the governing equations shown in Table 1. The Maxwell equation, for simplicity, was solved using the finite difference method. As mentioned before, σ depends only on the plasma temperature.

III.2 Numerical Method

The control volume is a special version of the weighted residuals method. This method consists on dividing the calculation domain in control volumes around grid points. The set of governing equations, or a single differential equation, is integrated over each control volume. This method guarantees the total conservation of quantities such as mass, momentum and energy.

The governing equations shown in Table 1 were solved iteratively using Patankar's control volume approach [17-19]. Although Patankar's method can present numerical diffusion and is less accurate than higher-order methods, it is highly stable and converges easily while the higher order methods tend to have convergence problems and use more computational time.

The numerical iteration procedure is described below:

1. Initial guess values for p, u, v, T, K and ε;
2. Plasma transport and thermodynamic properties are calculated for each grid point;
3. After solving equation 6, the current densities j_z and j_r can be obtained from equation 8. The azimuthal magnetic field is taken from the solution of equation 7;

4. Updated values of p, u, v, h (and consequently T), K and ϵ are obtained from the solution of their respectives equations presented in the Table 1;

5. Return to the second step and repeat the procedure until convergence is reached.

III.3 Computational Domain and Boundary Conditions

The computational domain used to solve the set of governing equations is shown in Fig.2. It is the upper half of a cross section of the plasma torch shown in Fig.1.

The computational domain is a simplified version of the plasma torch (Fig. 1), but it contains all the essential elements of that torch. Simplifications were conducted for computational reasons. The dimensions of the torch simulated in this work were chosen in order to represent a commonly used spraying torch.

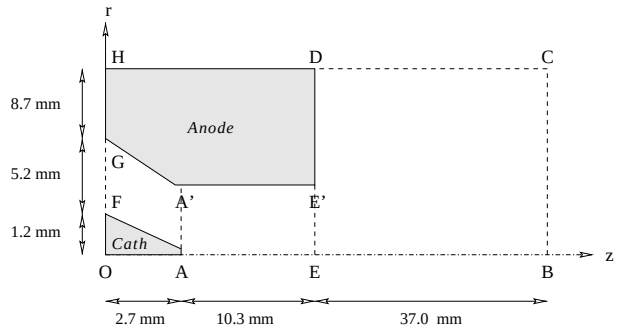

Figure 2. Computational domain of the plasma torch.

The gas is injected at FG. It flows through the torch until the electric arc region AA'EE', where the gas is heated. EBCD represents the region of free-boundary (outside the torch) and the line AB is the simmetry axis.

The boundary conditions assumed for the computational domain described in Fig.2 are the following.

1. Velocity.
   The axial velocity (u) at the entrance of the torch is determined specifing the gas flow rate. The radial velocity (v) is zero there. No-slip conditions are assumed in the electrodes region, i.e., $u = v = 0$. At the centre line AB, $\frac{\partial u}{\partial r} = v = 0$. Free-boundary conditions for BC and CD are assumed, $\frac{\partial(\rho u)}{\partial z} = \frac{\partial v}{\partial z} = 0$ and $u = \frac{\partial(r\rho v)}{\partial r} = 0$ respectively.

2. Enthalpy.
   The boundary conditions for enthalpy are given in terms of temperature and later converted into the enthalpy of the respective gas using equation 5. The temperature at the entrance of the torch and at CD are assumed to be equal to the room temperature ($\simeq 300\ K$). The surface of the cathode and of the anode are assumed to be at 3,000 K and 1,000 K, respectively (taken into consideration the interaction of the electric arc). In the centre line $\frac{\partial h}{\partial r} = 0$, and at BC $\frac{\partial h}{\partial z} = 0$.

3. Turbulence.
   The plasma flow is laminar at FG since the gas has not been heated by the electric arc yet; then K and ε are given by [16]

$$K_{in} = i_t(u^2 + v^2 + w^2) \quad and \quad \varepsilon_{in} = 3\frac{K_{in}^{3/2}}{R}\ , \tag{9}$$

where $i_t = 0.003$ is the turbulence intensity and R is the radius of the inlet to the nozzle. In the line AB, $\frac{\partial K}{\partial r} = \frac{\partial \varepsilon}{\partial r} = 0$ and at the free-boundaries BC and CD, $\frac{\partial K}{\partial z} = \frac{\partial \varepsilon}{\partial z} = 0$ and $K = \varepsilon = 0$, respectively. Near the anode region, a *wall-function* is used to obtain the values of K and ε (the laminar effects are quite significant there),

$$K_p = \frac{U_\tau^2}{\sqrt{C_\mu}} \quad and \quad \varepsilon_p = \frac{U_\tau^3}{\kappa_0 y_p}\ , \tag{10}$$

where $\kappa_0 = 0.41$ is the Von Kármán constant, U_τ is the resultant frictional velocity given by the *law of the wall*,

$$\frac{U_p}{U_\tau} = \frac{1}{\kappa_0}\ln\left(\frac{E\rho U_\tau y_p}{\mu}\right)\ , \tag{11}$$

where U_p is the parallel velocity to the wall, $E = 9.973$ is the roughness parameter for smooth walls, and y_p is the distance from point P to the wall.

4. Electrical Potential.
   The boundary condition for the electrical potential is determined assuming a current profile at line AA' [16,20],

$$j_z = j_0 e^{-r/r_c} \ , \qquad (12)$$

   where j_0 and r_c are constants which depend on the current. For a blunter cathode tip and $I = 200A$, $j_0 = 100Amm^{-2}$ and $r_c = 1.5mm$; for $I = 400A$, $j_0 = 130Amm^{-2}$ and $r_c = 2.5mm$. These values are not the same if a sharp cathode is used: j_0 is slightly higher and r_c smaller. In the line AB, $\frac{\partial j_z}{\partial r}$=$j_r$=0; j_r=j_z=0 in ED and $\Phi = 0$ at the anode.

A summary of the used boundary conditions is given in Table 3.

Table 2: **Boundary conditions used for the model**

	AB	BC	CD	FG	AA'	EE'	$Anode$	$Cathode$
u	$\partial u/\partial r = 0$	$\partial(\rho u)/\partial z = 0$	0	$u = cte$			0	0
v	0	$\partial v/\partial z = 0$	$\partial(r\rho v)/\partial r = 0$	0			0	0
h	$\partial h/\partial r = 0$	$\partial h/\partial z = 0$	$300K$	$300K$			$1,000K$	$3,000K$
K	$\partial K/\partial r = 0$	$\partial K/\partial z = 0$	0	K_{in}			k_p	
ε	$\partial \varepsilon/\partial r = 0$	$\partial \varepsilon/\partial z = 0$	0	ε_{in}			ε_p	
Φ	$\partial j_z/\partial r = j_r = 0$				j_{given}	$j_{r,z} = 0$	0	

IV. Results

The computer program was successfully tested in terms of iteration number and grid points. After 3,000 iterations for a grid with 100 points in the axial direction and 60 points in the radial direction, the temperature and velocity profiles remained unchanged even if a greater number of iterations or grid points were used. After the preliminary tests with the code, the results obtained in this work were compared with published ones. Examples of the temperature and velocity profiles, as well as the electrical potential and axial current density profiles, obtained using the computer code described previously and the torch shown in Fig. 2, are presented after the comparison with results from the literature.

IV.1 Comparisons

The results obtained from the computer code developed here were compared with the results obtained from other researchers. Unfortunately, experimental results for plasma velocities and temperatures inside the torch are extremelly difficult to be obtained due to the high temperatures and velocities found there.

The results of this work were compared with results obtained from numerical simulations. It is quite difficult to find numerical simulations that include the electric arc region. It is generally assumed a velocity and temperature profile at the nozzle exit, and using those profiles simulations for the behaviour of the plasma jet are conducted. The shortback of that method is obvious; the velocity and temperature profiles obtained depend entirely on the profiles initially assumed.

The only published results found by the authors that could be compared to the present work are the ones of Bauchire *et al* [21]. The plasma torch simulated in that work was similar to that of Fig.2; the dimensions of that torch were $9.1mm$ for the anode length and $3.4mm$ for the cross section of the torch; the operating conditions were $I = 100A$, gas flow rate of 3.4 l/min and argon was considered for both the plasma and the surrounding gas. Those were the same conditions and torch geometry reported by Bauchire *et al* [21], using a similar numerical method as the one used here.

The results obtained by Bauchire *et al* and in this work compare well, corroborating the assumption of the present model and the numerical method. Fig.3 shows the temperature and velocity profiles at the centre line obtained from the computer code developed here and from Bauchire *et al* [21]. The $0mm$ corresponds to the

beginning of the computational domain represented by the point O in Fig.2.

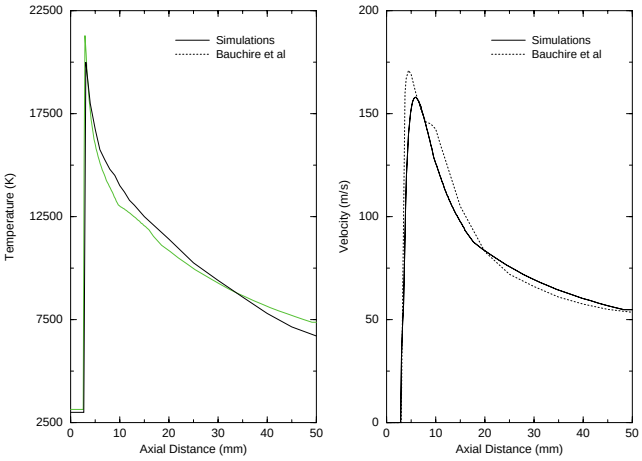

Figure 3. Temperatures and velocities at the centre line obtained from the present work (full line) and for Bauchire *et al* (dotted line).

The temperatures, as well as the plasma jet velocities, reach their maximum at the vicinity of the cathode ($\approx 3mm$) due to the high current density existing there. The differences between the results of the two studies can be attributed to different assumptions such as the energy transported by the electrons travelling to the anode, considered to be negligible compared with other terms of the energy equation in this work. Another reason for the differences could be the use of different values for the constants j_0 and r_c since they were not available in Bauchire *et al* [21].

IV.2 Turbulence

In Fig.4 we show the temperature and velocity profiles at the centre line for laminar and turbulent flow as obtained in this work.

It can be seen that turbulence effects were negligible. This conclusion is valid when using low current ($< 300A$), low gas flow rate ($< 50l/min$) and when the surrounding and the plasma gas are the same. Similar conclusions were also reached by Bauchire *et al* [21].

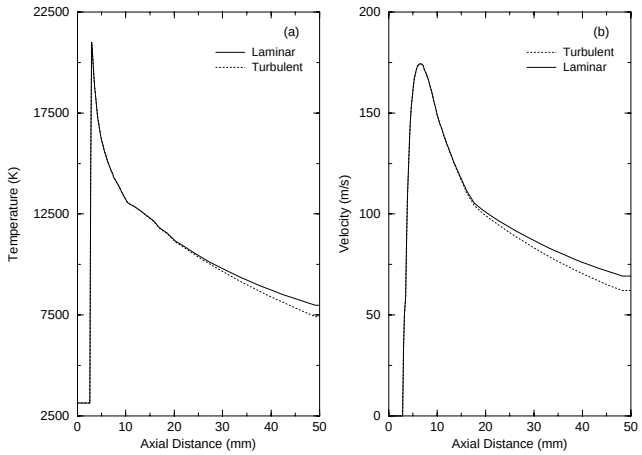

Figure 4. Temperatures (a) and velocities (b) at the centre line obtained for laminar (full line) and turbulent (dotted line) jet flow.

IV.3 Simulations of the non Transferred Plasma Torch

Examples of results obtained in this study are presented below. The gas was considered to be Argon for both the plasma and the surrounding gas. The plasma gas flow rate was 20 l/min and an electric arc of $100A$ was used for the examples given here. The cross section of the torch and the anode length are given in the computational domain. The temperature and velocity contours at the entrance of the torch, electric arc region and free boundary region for the conditions given above are shown in Fig.5. The outermost contour is $T = 2,000K$, the innermost contour is $T = 18,000K$ and the countour steps are $2,000K$; the outermost contour of the velocity is $20m/s$ and the innermost is $240m/s$; the contour steps are $20m/s$. We can see from Fig. 5 that the hotest and fastest region of the plasma jet is inside the torch. Someone using the plasma torch for spraying or treating residues can take advantage of the high temperatures and velocities of the plasma jet found inside the torch by injecting the particles with the working gas.

The highest temperature and velocity occur in the axis of the torch. The centre line profiles of the velocities and temperatures of the plasma jet are shown in Fig.6.

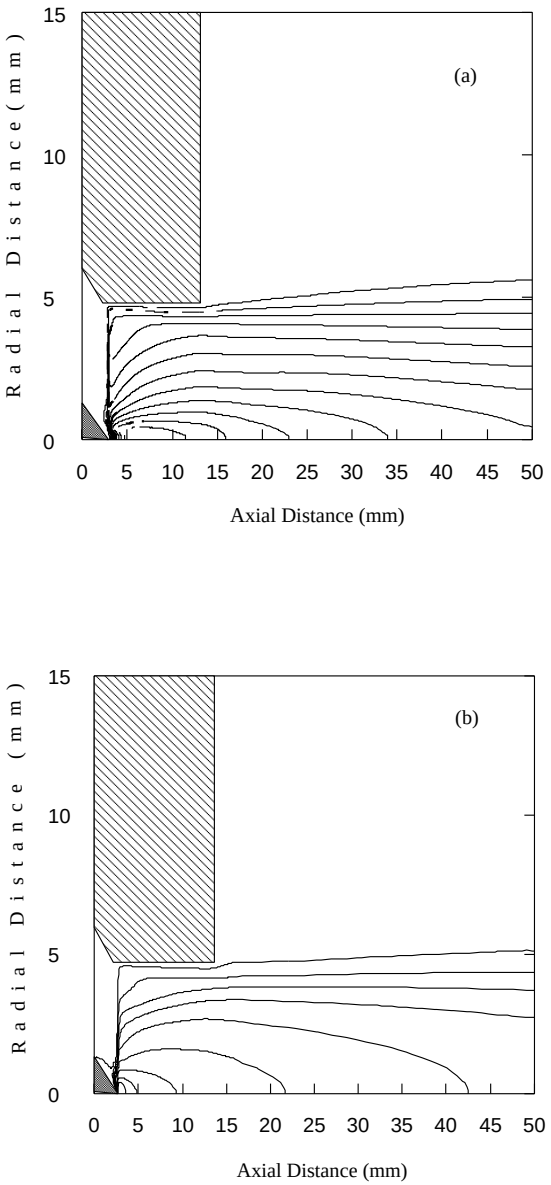

Figure 5. Velocity (a) and temperature (b) contours of the plasma flow in the torch. The outermost contours are $2,000K$ and $20m/s$ and the innermost are $18,000K$ and $240m/s$. The contour steps are $2,000K$ and $20m/s$.

Near the cathode tip, the temperature reaches its maximum around $21,000K$; at the torch exit ($\approx 13mm$) $T = 13,500K$ and after $50mm$, the temperature drops to $9,500K$. The maximum velocity is reached near the cathode tip similarly to what was observed for the temperature; the value of the velocity is around $260m/s$ there and at the torch exit, the plasma jet velocity at the center line is $240m/s$; at the end of the computational domain the velocity is aproximately $160m/s$.

The temperature decays faster inside than outside the torch. This behaviour is probably due to the electrodes cooling (inside the torch) while in the free boundary region (outside the torch) the plasma jet cools off influenced only by the surrounding gas.

Fig. 7 presents the radial temperature distribution at different axial positions. The temperature decays very quickly in this direction reaching values near the room temperature at $r = 5mm$ (nozzle diameter).

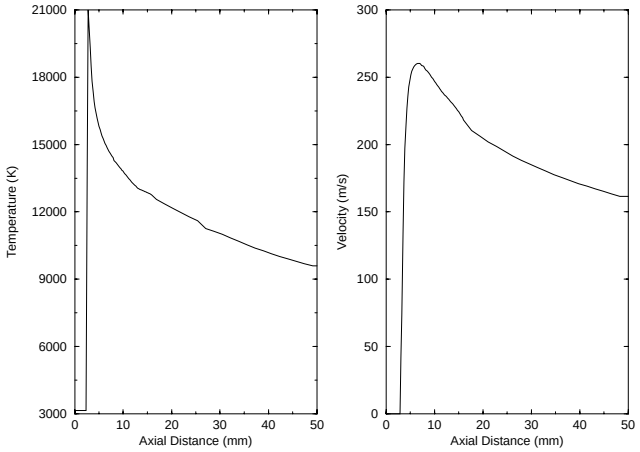

Figure 6. Temperature and velocity profiles at the centre line for a plasma torch of 20 l/min of gas flow rate and $I = 100A$ simulated in this work.

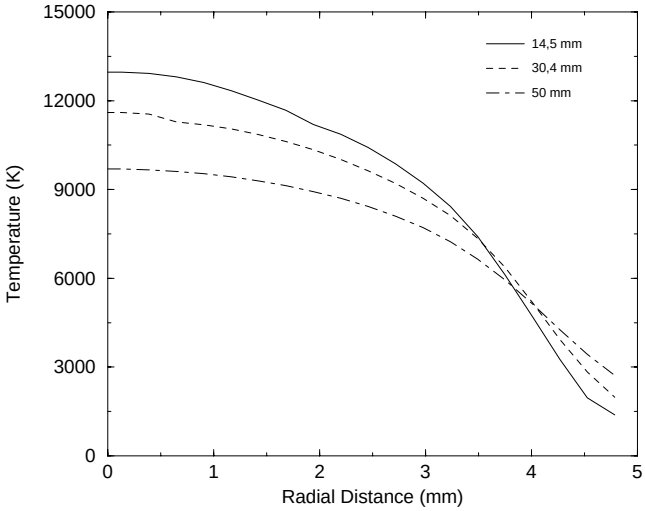

Figure 7. Radial profile of temperature of the torch in different axial positions. $z = 14.5mm$ (full line), $z = 30.4mm$ (dashed line) and $z = 50mm$ (dot-dashed line).

It is observed that the temperature lines for different axial positions in Fig.7 cross at a radial distance of approximately $3.5mm$. This behaviour is probably

caused by the failure of the L.T.E. assumption for temperatures below $9,000K$ and has been reported by other researchers [10,22,23].

The computer code developed in this work calculates also the electrical potential of the plasma. The value of the electrical potential for the operating conditions given above was around $13V$, not including the anode and cathode falls. The electrodes fall should add to the electrical potential a value between 10 and $15V$ [7-9]. Plasma torches using Argon, with geometries and operating conditions similar to the ones simulated here, have overall voltages between 20 and 30 V, in agreement with the results obtained here.

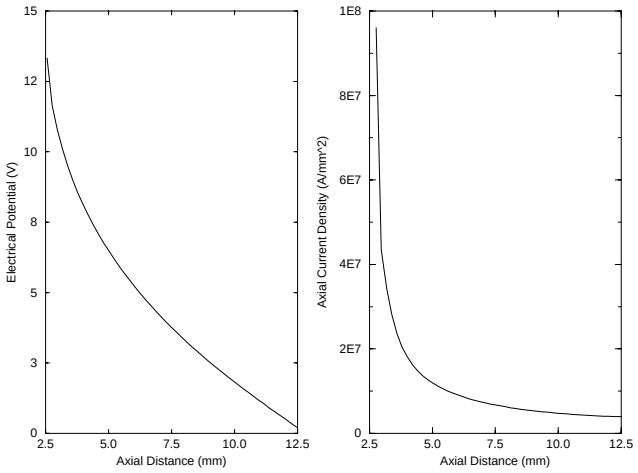

Figure 8. Electrical potential and axial current density at the centre line of the torch.

The axial coordinate in Fig.8 starts at a distance of $2.5mm$ which coincides with the cathode tip. The axial current density shows an exponential behaviour and its maximum value occurs exactly at the cathode tip resulting on the increase of the plasma temperature to its maximum value as mentioned before.

V. Conclusion

We have developed physical and mathematical models to simulate the plasma flow through the torch, including the regions of the gas entrance and electric arc besides the free boundary region. The equations of the model were numerically solved using the control volume formulation of Patankar.

The computer code was tested and showed great flexibility, allowing easy modification of the torch geometry and operating conditions such as arc current and gas flow rate.

The results obtained from the computer program were initially compared with published data showing good agreement. Examples of temperature and velocity profiles for the torch simulated in this work were given, indicating that the highest temperature occurs inside the torch and its value is around $21{,}000K$. The velocity profile shows a similar behaviour observed for the temperature, with a maximum value of $260m/s$. It was also seen that those profiles (temperature and velocity) decay faster inside the torch; this fact is probably due to the influence of the cooling of the electrodes.

Acknowledgement

Financial support from CNPq and FAPESP through a scholarship for R. C. Favalli is gratefully acknowledged.

References

1. J. Szekely and D. Apelian, "Plasma process in synthesis of materials," in *MRS Symposium Proceedings* (Anaheim), 1987.
2. EPRI Workshop, *Research Opportunities for Plasma Processing*, (Palo Alto), 1987.
3. R. N. Szente, "Industrial applications of thermal plasmas," in *AIP Conference Proceedings*, vol. 345, (Paraná, BR), p. 487, 1995.
4. R. N. Szente, "Internal report," Tech. Rep. 217/94, Canadian Electrical Association, 1994.
5. Y. C. Lee, *Modelling Work in Thermal Plasma Processing.* PhD thesis, Mechanical Engineering, University of Minnesota, Minnesota, USA, 1984.
6. A. Mazza, *Studies of an Arc Plasma Reaction for Thermal Plasma Synthesis.* PhD thesis, Mechanical Engineering, University of Minnesota, Minnesota, USA, 1983.
7. E. Pfender, *Electric Arcs and Arc Gas Heaters.* USA: Hirsh and Oskam Inc., 1978.
8. E. R. G. Eckert and E. Pfender, *Advances in Plasma Heat Transfer.* Minnesota, USA: University of Minnesota, 1967.
9. J. Feinman, *Plasma Technology in Metallurgical Processing.* Grand Junction, USA: J. Feinman and Associates, 1987.
10. D. A. Scott, P. Kovitya, and G. N. Haddad, J. Appl. Phys. **66**, 5232 (1989).
11. B. E. Launder and D. B. Spalding, "The numerical computation of turbulent flows," *Computer Methods in Applied Mechanics and Engineering*, **3**, 269 (1974).

12. B. E. Launder and D. B. Spalding, *Mathematical Models of Turbulence.* London, UK: Academic Press Inc., 1972.
13. S. Paik, G. Hawkes, and H. D. Nguyen, "Effect of working gases on thermal plasma waste treatment," Plasma Chemistry and Plasma Processing **15**, 677 (1995).
14. M. I. Boulos, 1996. Private Communication, University of Sherbrooke, Canada.
15. J. J. Lowke, P. Kovitya, and H. P. Schmidt, J. Phys. D: Applied Physics **25**, 1600 (1992).
16. A. B. Murphy and P. Kovitya, J. of Appl. Phys. **73**, 4759 (1993).
17. S. V. Patankar, *Numerical Heat Transfer and Fluid Flow.* New York, USA: McGraw Hill, 1980.
18. S. V. Patankar, "A numerical method for conduction in composite materials, flow in irregular geometries and conjugate heat transfer," in *Proceedings of the 6th International Heat Transfer Conference*, (Toronto, Canada), p. 297, 1978.
19. S. V. Patankar, Journal of Numerical Heat Transfer, **4**, 409 (1981).
20. K. C. Hsu, K. Etemadi, and E. Pfender, J. of Appl. Phys. **54**, 1293 (1983).
21. J. M. Bauchire, J. J. Gonzalez, and A. Gleizes, "A physical modelling of a dc plasma torch," in *Proceedings of 12th ISPC,* vol. **3**, (Minnesota, USA), p. 1761, 1995.
22. J. D. Ramshaw and C. H. Chang, Plasma Chemistry and Plasma Processing, **12**, 299 (1992).
23. A. H. Dilawari, J. Szekely, J. Batdorf, R. Detering, and C. B. Shaw, Plasma Chemistry and Plasma Processing, **10**, 321 (1990).